JOURNAL OF MATERIALS SCIENCE 22 (1987) 2645–2654

The thermal reactions of muscovite studied by high-resolution solid-state 29–Si and 27–Al NMR

K. J. D. MACKENZIE, I. W. M. BROWN, C. M. CARDILE, R. H. MEINHOLD
Chemistry Division, D.S.I.R., Private Bag, Petone, New Zealand

Studies of two muscovites of different iron contents, using solid-state NMR with magic-angle-spinning (MAS) combined with X-ray powder diffraction, thermal analysis and ^{57}Fe Mössbauer spectroscopy, suggest that dehydroxylation occurs by a homogeneous rather than an inhomogeneous mechanism, forming a dehydroxylate in which the aluminium is predominantly 5-coordinate. On further decomposition at about 1100° C, the tetrahedral layer and interlayer K^+ form a feldspar-like phase similar to leucite ($KAlSi_2O_6$), the remainder forming a spinel, which, contrary to previous suggestions, appears to contain little silicon. Further heating induces the formation of mullite ($Al_6Si_2O_{13}$), and, in the higher-iron sample, corundum (α-Al_2O_3), in addition to the feldspar-like phase. The presence of the iron impurity enhances the recrystallization reactions and promotes the conversion of mullite to corundum, which eventually becomes the sole aluminous product in the high-iron sample. In samples fired to higher temperatures, only the tetrahedral aluminium resonance is detectable by ^{27}Al NMR, probably because most of the iron is located in either the mullite or corundum phases, in which it broadens the octahedral aluminium resonance beyond detection.

1. Introduction

The commonly-occurring mica mineral muscovite is a 2:1 dioctahedral hydroxy aluminosilicate, named after its type location, the Russian province formerly called Muscovy. In ideal muscovites, $K_2Al_4(Si_6Al_2)O_{20}(OH)_4$, the octahedral sites are occupied exclusively by aluminium, with appreciable tetrahedral Al-for-Si substitution also occurring, charge balance being achieved by the presence of the potassium ions in the interlayer positions (Fig. 1a).

Muscovite occurs in both a finely-divided form, as a common accessory mineral in ceramic clays, and in a massive tabular form, in which it finds a number of applications. In addition to its practical importance, its high degree of crystallinity suggests that it might be an ideal subject for fundamental studies, particularly of structural changes accompanying the high-temperature reactions.

When heated, muscovite loses its hydroxyl water at about 750° to 950° C, the precise temperature depending on the state of subdivision, chemical composition and the water vapour pressure of the reaction atmosphere [1]. The X-ray pattern of the dehydroxylated phase is similar to that of unheated muscovite, even though the conversion of two hydroxyls to one oxygen must cause considerable changes in the environment of the octahedral cations. Eberhart [2] proposed two possible structures for the dehydroxylate, computer simulations of which are shown in Fig. 1.

In one structure (Fig. 1b), the residual hydroxyl oxygens are considered to remain in their original plane whereas in the second possibility, considered by Eberhart to be more consistent with the results of his one-dimensional Fourier analysis [2], the residual oxygens are moved into the plane of the octahedral aluminium. Although Eberhart's schematic diagrams [2] suggest 5-coordinate aluminium in both structures, his further attempts to rationalise this second structure are not consistent with this schematic concept, being based instead on an erroneous structure for montmorillonite dehydroxylate proposed by Bradley and Grim and discussed in [8]. The deficiencies of this structure are also apparent from the computer simulation of the muscovite dehydroxylate structure eventually deduced by Eberhart [2] (Fig. 1c), in which the aluminium is formally 6-coordinate, but with the two bridging Al–O distances impossibly long for bonding (0.26 nm). A more recent 3-dimensional Fourier study of muscovite dehydroxylate by Udagawa *et al.* [3] indicates a structure containing 5-coordinate aluminium with the bridging residual oxygens in the plane of the aluminium, consistent with Eberhart's schematic concept rather than the more formalized Eberhart/Bradley/Grim structure.

The formation of dehydroxylate structures of this type implies the elimination of pairs of hydroxyl groups in close proximity (the so-called homogeneous mechanism). An alternative inhomogeneous mechanism has been proposed by Nicol [4], involving migration of Al^{3+} through a relatively fixed oxygen lattice to "acceptor" regions which eventually form crystalline products, and a counter-migration of protons to "donor" regions from which water is lost, forming pores. Although Nicol did not work out the details of

0022–2461/87 $03.00 + .12

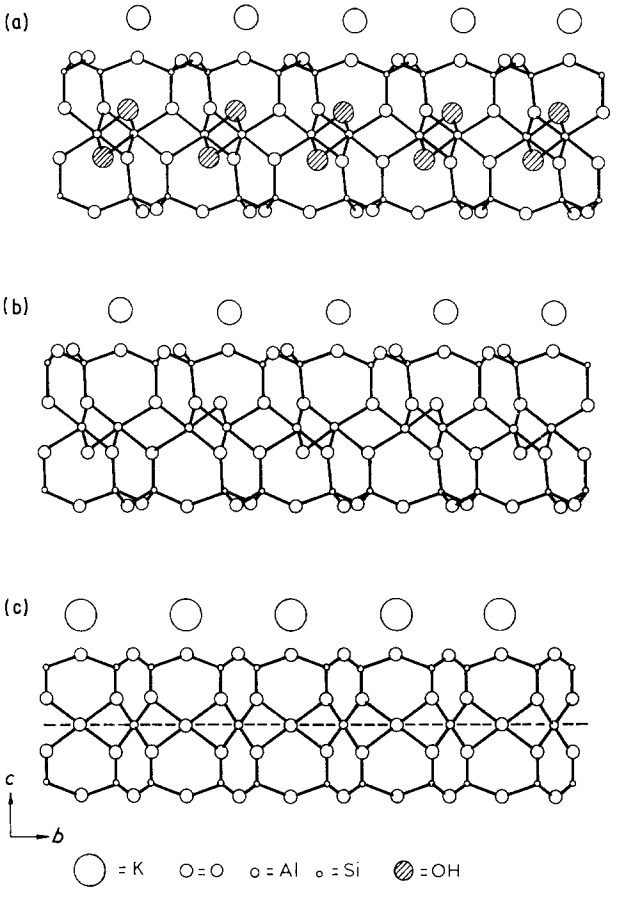

Figure 1 Computer-generated structural diagrams of muscovite and previously-suggested muscovite dehydroxylate structures. Views along the *a*-axis. (a) Muscovite, after Radoslovich [19], (b) Muscovite dehydroxylate, based on a suggestion by Eberhart [2], (c) Muscovite dehydroxylate, adapted by Eberhart from a concept of Bradley and Grim. Broken lines indicate postulated metal–oxygen bonds too long to be within practical bonding distance.

such a reaction, the effect is to preserve the original oxygen configuration in the acceptor regions i.e. maintaining 6-coordinate aluminium, facilitating the transformation of these regions to a phase designated [4] Phase I. A further implication of the inhomogeneous mechanism is the counter-migration of K^+ to the donor regions, which eventually form leucite, $KAlSi_2O_6$, or sanidine, $KAlSi_3O_8$.

When heated to $> 1000°$ C, the X-ray reflections of the dehydroxylate are progressively replaced by those of a cubic intermediate phase, variously identified as γ-Al_2O_3 [5] or a Si–Al spinel, $Si_8(Al_8\square_8)(O_{28}\square_4)$ [2]. Nicol [4] has suggested that his Phase I is an intermediate between muscovite dehydroxylate and this spinel.

The high-temperature products are said to be dependent on the composition of the starting material, particularly its Si : Al ratio [1] and the amount of substitutional iron present; low-iron muscovites form mullite in addition to leucite, whereas higher-iron samples form corundum rather than mullite [6].

The outstanding questions concerning the thermal reactions of muscovite may be summarized thus:

(a) What is the structure of the dehydroxylate, and does its structure depend in any way on the chemical nature of the starting material?

(b) Does the dehydroxylate form by a homogeneous or inhomogeneous mechanism?

(c) How does the nature of the starting material influence the structure and formation mechanism of the higher-temperature intermediate phases and final products?

In the present work, these questions are addressed using high-resolution solid-state ^{29}Si and ^{27}Al NMR with magic-angle spinning (MAS), in conjunction with thermal analysis, Mössbauer spectroscopy and X-ray powder diffraction, a combination of techniques which has proved useful in studying the thermal reactions of the related minerals pyrophyllite [7] and montmorillonite [8].

2. Experimental procedure

Two muscovites were studied here; one, from Point Pegasus, Stewart Island, New Zealand (New Zealand Geological Survey sample 8299) contains 3.2% Fe and forms corundum and leucite on prolonged heating at 1250° C, whereas the other muscovite, from Mitchell County, North Carolina, USA, contains only 1.7% Fe and forms mullite at 1250° C. The iron contents of both muscovites are sufficient to allow Mössbauer spectroscopy to be carried out. The chemical analyses and unit cell compositions of the two muscovites are given in Table I. The X-ray traces of both muscovites indicate well-crystallized samples of the stable monoclinic $2M_1$ polytype structure, with no impurity phases detectable. Thermal analyses were carried out in ambient air on 5 mm square flakes at a heating rate of $10°\,C\,min^{-1}$. The NMR experiments were carried out on similar flake samples, heated in platinum-lined ceramic boats, at temperatures chosen with reference to the thermal analysis results. With the exception of the 1250° C experiments, all the heatings were of 15 min duration, after which the flakes were lightly ground in an agate mortar to pass a 152 μm sieve. The

TABLE I Chemical analysis and unit cell formulae of the muscovites using in this study

	North Carolina	Stewart Island	Ideal
SiO_2	44.65	43.29	45.2
Al_2O_3	35.00	34.66	38.4
Fe_2O_3	2.43	4.59	–
MgO	1.40	0.86	–
CaO	–	–	–
Na_2O	0.95	0.79	–
K_2O	11.05	11.05	11.8
H_2O^+	4.40	4.60	4.5
Total	99.88	99.84	99.9
Unit cell contents, based on 24(O, OH)			
Si	6.00 } 8.00	5.86 } 8.00	6.0 } 8.0
Al	2.00 }	2.14 }	2.0 }
Al	3.54 }	3 38 }	4.0 }
Mg	0.28 } 4.06	0.17 } 4.01	– } 4.0
Fe^{3+}	0.24 }	0.46 }	– }
K	1.90 } 2.14	1.91 } 2.11	2.0 } 2.0
Na	0.24 }	0.20 }	– }
OH	3.94	4.16	4.0
O	20	20	20

Analysts: G. D. Walker and R. R. Exley.

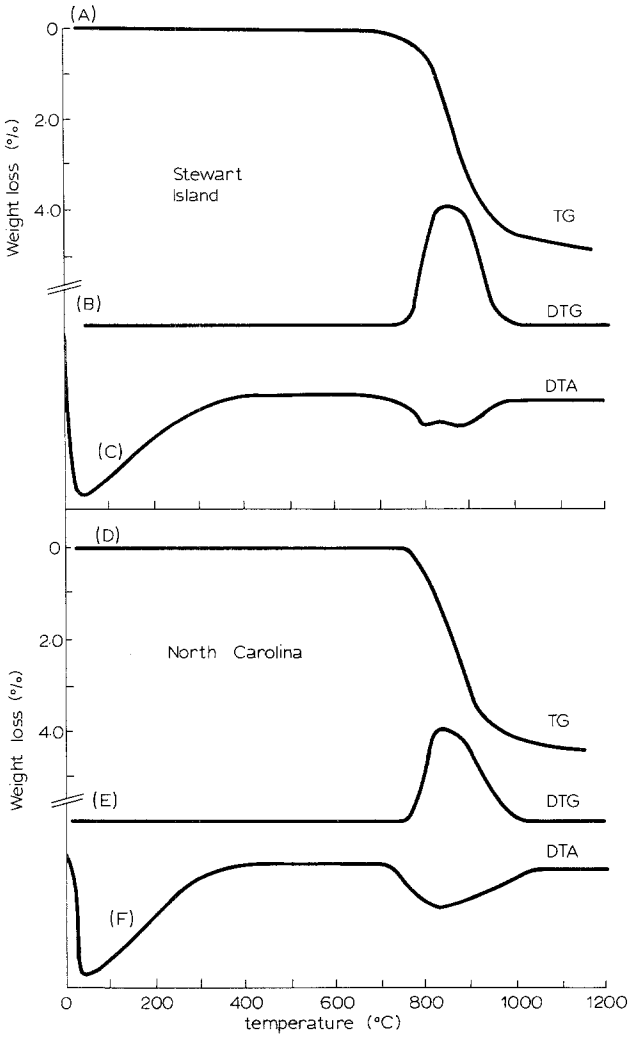

Figure 2 Thermal analysis curves of muscovites, heating rate 10° C min^{-1}, in static air. TG = thermogravimetric curve, DTG = differential thermogravimetric curve, DTA = differential thermal analysis curve.

NMR measurements were made using a Varian XL-200 spectrometer at MAS speeds of 2 to 2.5 kHz. Precise X-ray measurements of the unit cell parameters were also made, using elemental silicon powder as an internal angular calibration standard. The Mössbauer measurements were made using Elscint AME 50 and Cryophysics spectrometers with Co–Rh sources referenced to natural iron and the spectra were computer-fitted to Lorentzian lineshapes. Further details of the NMR and Mössbauer experimental procedures are given elsewhere [8].

3. Results and discussion

3.1. Thermal analysis and X-ray diffraction of muscovites

The thermal analysis curves are shown in Fig. 2. The curves for both muscovites are similar, and are consistent with those of massive samples [9]. By contrast, finely-divided samples absorb ambient moisture which is gradually evolved over a temperature range, overlapping with the gradual loss of hydroxyl water, the resulting differential thermal analysis trace being devoid of thermal peaks [9]. For this reason the present heatings were carried out using massive samples to allow the reaction to be reproducibly related to discrete events on the thermal curves. The initial low-temperature endotherm (Fig. 2, C and F), which is not associated with a detectable weight loss, is an artifact of initial baseline drift. Both muscovites show similar dehydroxylation weight losses of ~4.5%, beginning at 700° C and extending over a range of about 250° C (Fig. 2, A and D). This event is detected by DTA as a broad, weak endotherm which in the Stewart Island sample is partially resolved into two overlapping peaks (Fig. 2, C). The X-ray patterns of both micas are unchanged up to the onset of dehydroxylation, which is accompanied by a ~2.6% expansion of the measured cell volume and changes in the intensities of the muscovite peaks. The X-ray patterns of both muscovites partially dehydroxylated by heating to 800° C show both the muscovite and muscovite dehydroxylate reflections, indicating that the two phases can coexist during dehydroxylation. On the completion of dehydroxylation at 950° C, only the dehydroxylate reflections remain, but by 1100° C, these reflections have also disappeared, with the appearance of several new weak reflections corresponding to cubic phases of a = 0.7963 nm and a = 0.7949 nm in the North Carolina and Steward Island samples, respectively. These compare well with the lattice parameter of the spinel phase reported by Eberhart (0.797 nm) [2]. No further thermal events are observed in the thermal analysis curves within the temperature range of the present experiments. This is consistent with the X-ray result that recrystallization of the high-temperature phases is slow, even at 1250° C. Heating the Stewart Island sample for 2 h at 1250° C results in the appearance of a feldspar-like phase, corundum (α-Al_2O_3) and a small amount of mullite. The feldspar-like phase exhibits a number of the X-ray reflections of leucite, suggesting that this phase is related to leucite, but there are a number of differences in the X-ray pattern which preclude its confident identification. Precise X-ray measurements of the mullite cell parameters indicate, on the basis of Cameron's relationship between the *a*-parameter and the unit cell volume [10], that this phase contains ~6.5% Fe_2O_3. Taking into account this iron content, Cameron's relationship indicates that this mullite contains 64.9 mol % Al_2O_3, i.e. it is a rather aluminous mullite of composition intermediate between 2 : 1 (66.6 mol % Al_2O_3) and 3 : 2 (60.0 mol % Al_2O_3). This mullite disappears on longer heating at 1250° C, the final products being the crystalline feldspar-like phase and corundum. The cell parameters of the latter are not significantly changed by the prolonged heating, and indicate a unit cell volume ~0.9% greater than that of pure α-Al_2O_3. On the basis of the data of Muan and Gee on the relationship between the corundum lattice parameter and the degree of Fe_2O_3 in solid solution [11], the present corundum is estimated to contain 9.4 wt % Fe_2O_3, i.e. a considerable proportion of the original iron is concentrated in this phase. The changes in the relative X-ray intensities of the high-temperature phases of both muscovites during heating are shown in Fig. 3.

Recrystallization occurs much more slowly in the North Carolina muscovite than in the Stewart Island material; samples heated for 2 h at 1250° C still

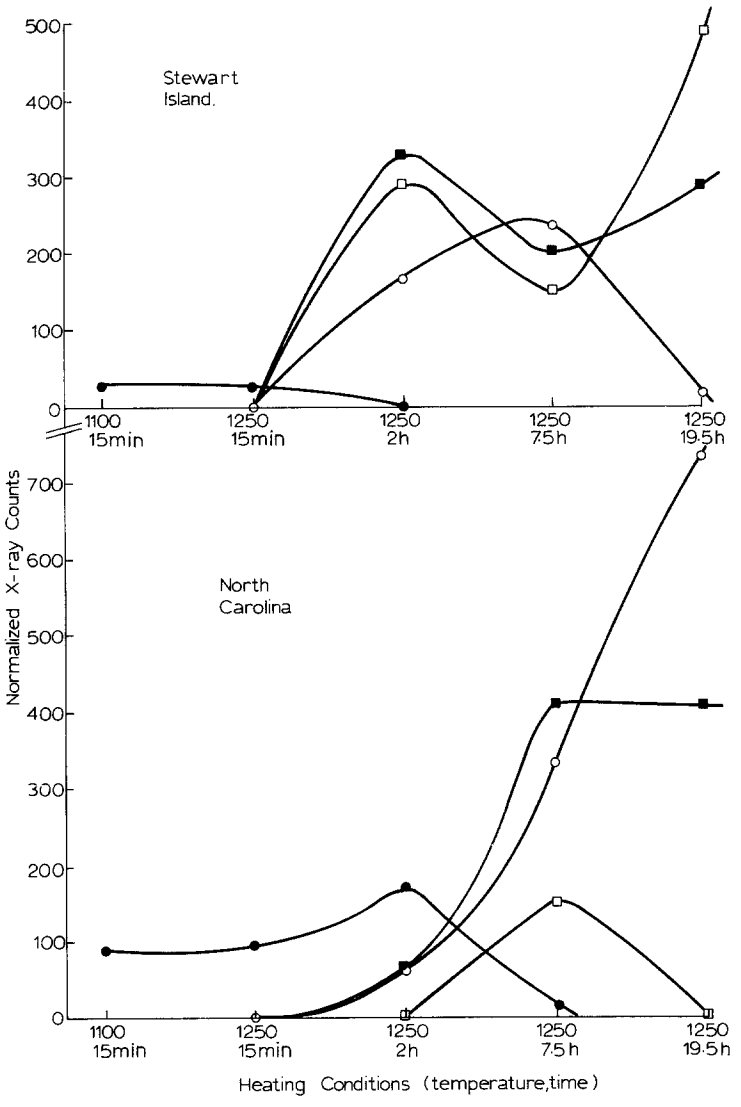

Figure 3 Changes in the relative X-ray intensities of the high-temperature phases with heating conditions. Reflections used: (●) spinel, 0.240 nm, (○) mullite 0.340 nm, (■) feldspar-like phase, 0.329 nm, (□) corundum, 0.209 nm.

contain X-ray peaks of the spinel, in addition to new reflections corresponding to very poorly crystalline mullite and leucite-like feldspar. More prolonged heating at 1250° C causes the spinel reflections to disappear and the feldspar-like phase and mullite to become more crystalline. Precise cell parameter measurements of the latter indicate that it contains at least 3% Fe_2O_3, estimated from Cameron's relationship [10]. When initially detected after 2 h firing at 1250° C, the composition of this mullite, although difficult to measure because of its poor crystallinity, is estimated from the cell parameters corrected for the iron content [10] to be highly aluminous (68.4 mol % Al_2O_3). After more prolonged heating at 1250° C, the composition becomes less alumina-rich (65.8 mol % Al_2O_3, i.e. closer to 2 : 1 mullite than 3 : 2). A similar progressive trend towards a more silica-rich mullite composition on heating has also been reported in the thermal decomposition sequence of kaolinite [12].

3.2. NMR spectroscopy

Typical ^{29}Si NMR spectra are shown in Fig. 4. The spectra of the unheated muscovites (Figs 4A and D) show large spinning sidebands and a broadened centreband (width ~ 20 p.p.m.), due to the presence of paramagnetic iron, the effect being more pronounced in the Stewart Island sample, which has the higher iron content. The chemical shift of unheated Stewart Island and North Carolina samples (−86 p.p.m.) is in agreement with those previously reported for muscovites (−84.6 to −86.7 p.p.m. [14], −86 p.p.m. [15] and −85 p.p.m. [13]). Sanz and Serratosa, using a low-iron sample, resolved two weaker additional resonances at −89 and −81 p.p.m. which they assigned to $Si(Si_3)$ and $Si(SiAl_2)$ environments, the principal resonance at −85 p.p.m. being assigned to $Si(Si_2Al)$ [13]. These weaker resonances were not observed by other workers, nor were they seen in the present study, either because of peak broadening and poorer resolution or because the tetrahedral aluminium is fully ordered within the tetrahedral lattice, a situation which has been shown by theoretical modelling [16] to give rise to only the single (Si_2Al) resonance.

The ^{29}Si spectra are unchanged by heating to 650° C, but the onset of dehydroxylation in Stewart Island muscovite is accompanied by a change in the ^{29}Si chemical shift to −89 p.p.m. (Fig. 4B). A corresponding change in the chemical shift of North Carolina muscovite becomes apparent only when dehydroxylation is largely complete at 950° C (Fig. 4E). The collapse of the dehydroxylate structure at 1100° C is accompanied by a further change in the ^{29}Si chemical shift to −99 ± 2 p.p.m. in both muscovites (Figs 4C and F). This chemical shift then remains unchanged throughout the high-temperature recrystallization

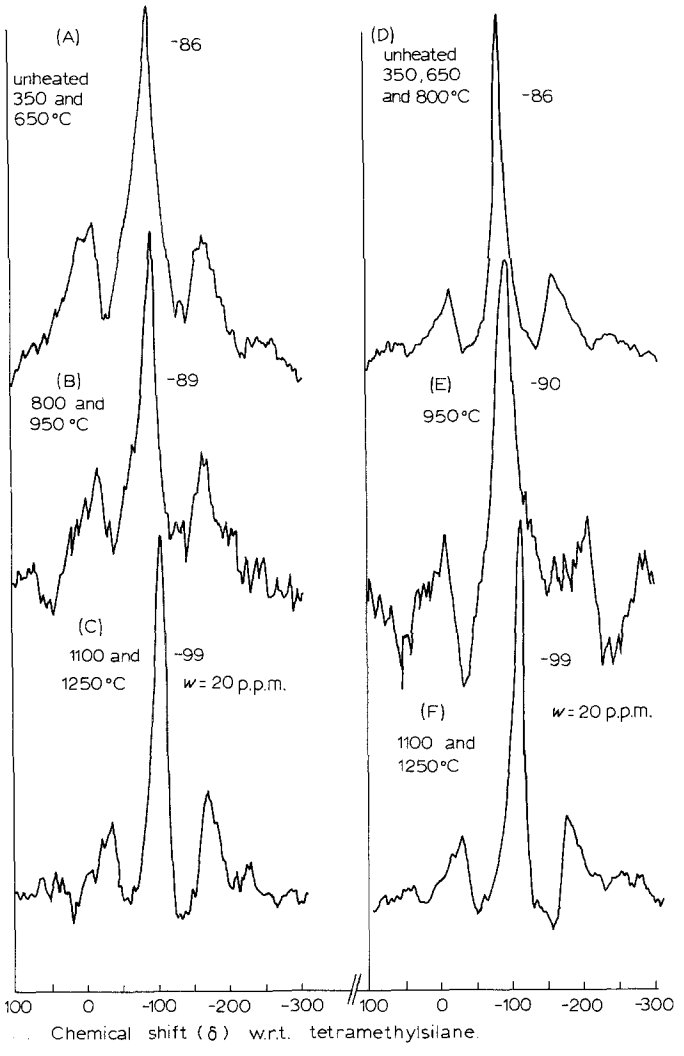

Figure 4 Typical ^{29}Si NMR spectra of muscovites heated to various temperatures. (A to C), Stewart Island muscovite, (D to F) North Carolina muscovite.

reactions, indicating that at no stage is free silica (either amorphous or crystalline) evolved, since such species have chemical shifts of -108 to -110 p.p.m. [8]. The ^{29}Si chemical shifts of the high-temperature samples are in the range reported for the various forms of the $KAlSi_3O_8$ feldspars, sanidine (-97, -101 p.p.m. poorly resolved [17]), orthoclase (-95 to -100 p.p.m., poorly resolved [18]) and microcline (-94.5, -96.8 and -100.2 p.p.m., well resolved [18]). The present single broad ^{29}Si resonance is more typical of a potassium feldspar which has been cooled from high temperature, in which the tetrahedral aluminium and silicon atoms are relatively disordered, [18] but the presence of iron may also contribute to the broadening. The ^{29}Si spectrum of the secondary aluminosilicate phase mullite, formed in North Carolina muscovite, should have a chemical shift of -88 p.p.m. [12] and would therefore be obscured by the 20 p.p.m. peak broadening of the present spectra centred near -100 p.p.m., since this phase contains a relatively small proportion of the total silicon.

The empirical relationship [7] between the ^{29}Si chemical shift δ and the mean Si–O–Si(Al) bond angle θ:

$$\delta = -176.65 - 55.821 \text{ Sec } \theta \qquad (1)$$

has been found to be valid for a number of other silicates and aluminosilicates, including layer-lattice minerals [7, 8, 12]. Several modern crystal structure determinations have been published [3, 19–21] for muscovites from various localities, having a range of chemical compositions. By substituting the atomic coordinates for each structure, together with unit cell data measured for the present samples, into a computer programme which calculates all the bond angles and distances [22], values of θ based on all the published structures were obtained, from which values of δ were calculated by Equation 1. All the structures predict a 1 to 2 p.p.m. difference in δ for the two crystallographically distinct silicons, but such differences cannot be experimentally resolved in the present spectra. The chemical shifts calculated for the various structures are similar, ranging from -86.3 to 90.2 p.p.m. but the structure of Radoslovich, [19] determined for a muscovite of almost identical chemical composition to the present North Carolina sample, predicts the chemical shift observed in this work (-86 p.p.m. for both unheated muscovites).

A similar calculation for muscovite dehydroxylate, made by substituting the measured parameters of the present dehydroxylated muscovites into the dehydroxylate structure of Udagawa *et al.* [3], predicts ^{29}Si chemical shifts of -96.7 to -97.9 p.p.m. by comparison with observed values of -89 to -90 p.p.m. This engenders confidence in the tetrahedral configuration of the Udagawa dehydroxylate structure, but suggests that the mean tetrahedral bond angles are about 5° smaller in the present dehydroxyl-

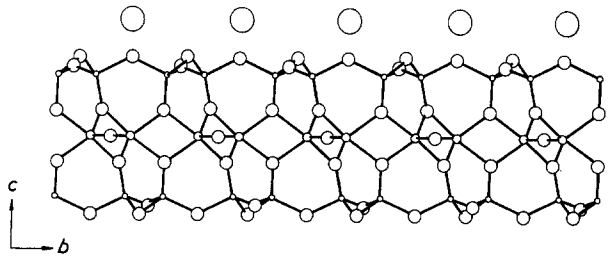

Figure 5 Computer-generated structure of muscovite dehydroxyate, based on Udagawa *et al.* [3], revised according to the present ^{29}Si NMR and X-ray data.

ates. Very small adjustments in the z-coordinates of the silicon atoms and their associated oxygens result in the dehydroxylate structure shown in Fig. 5, which has calculated δ-values of -89.1 and -90.6 p.p.m. If, as suggested by Eberhart [2], the spinel which appears following the breakdown of muscovite dehydroxylate contains silicon, its mean tetrahedral bond angle, which is independent of its cell parameter, predicts a ^{29}Si chemical shift of -80 p.p.m. [12]. Such a resonance is not clearly evident in the spectra of any of the spinel-containing samples; provided the ^{29}Si resonance of this phase is not being completely eliminated by the high concentrations of iron, which does not appear likely, this result suggests that the concentration of silicon in the spinel phase is considerably less than suggested by Eberhart's formulation, and may not be present at all.

In previous NMR studies of mineral dehydroxylation [7, 8, 12], useful additional information about the environment of the silicon atoms in proximity to hydroxyl protons was provided by cross-polarization (CP) measurements. Attempts were made to obtain CP spectra from the present muscovites, using a wide range of recycle delays and CP contact times, but the signals obtained were too weak to be useful. A possible inference is that the paramagnetic iron present interacts strongly with the protons, reducing the transfer of magnetization from protons to silicons. The effect on the silicon, which is seen in the broadening of the peak and the production of large spinning sidebands, is much less pronounced than the apparent effect on the proton system. This may indicate that the iron is preferentially incorporated into the octahedral sites where it is closer to the hydroxyls than to the silicons.

Typical ^{27}Al NMR spectra are shown in Fig. 6. Intensity measurements of the ^{27}Al resonance, calibrated with respect to α-Al_2O_3 (Fig. 7) indicate not all the Al in the muscovites is detected by NMR. A similar result was found for other layer-lattice aluminosilicates [7, 8], in which it was partly attributed to the broadening beyond detection of the signal from those aluminiums adjacent to iron atoms. The concentration of detectable aluminium decreases still further on dehydroxylation (Fig. 7), a phenomenon also observed in related minerals and attributed to the formation of 5-coordinate aluminium, which in these minerals is apparently broadened beyond detection by ^{27}Al NMR [7, 8]. Fig. 6 indicates that below the dehydroxylation temperature, the ^{27}Al spectra contain two resonances, at about 0 and 60 p.p.m., corresponding to aluminium in octahedral and tetrahedral sites respectively [23]. The relative occupancy by detectable aluminium of the octahedral and tetrahedral sites, estimated from the peak areas, is approximately 50% in each site. The detectable octahedral sites are thus underestimated, since the chemical analyses (Table I) suggest a tetrahedral aluminium content of only 36 to 38%. The loss of octahedral aluminium signal is again consistent with the presence of iron in predominantly octahedral sites. The detectable tetrahedral/octahedral aluminium ratio does not change significantly until dehydroxylation is complete (Fig. 6), whereupon the octahedral site can no longer be detected, and the chemical shift of the tetrahedral site decreases. Since at least one of the Al-containing product phases present in each of these muscovites (corundum or mullite) contains a significant proportion of octahedral aluminium, this unexpected result suggests that the aluminium signal from these phases is being lost, possibly because they preferentially take up iron, as indicated by the X-ray measurements of the corundum and mullite lattice parameters. The other Al-containing product common to both muscovites is the potassium feldspar-like phase, which contains only tetrahedral aluminium. Reported ^{27}Al spectra for related potassium feldspars contain a tetrahedral resonance at 54 to 58 p.p.m. [17], consistent with the present spectra of the higher-fired muscovites.

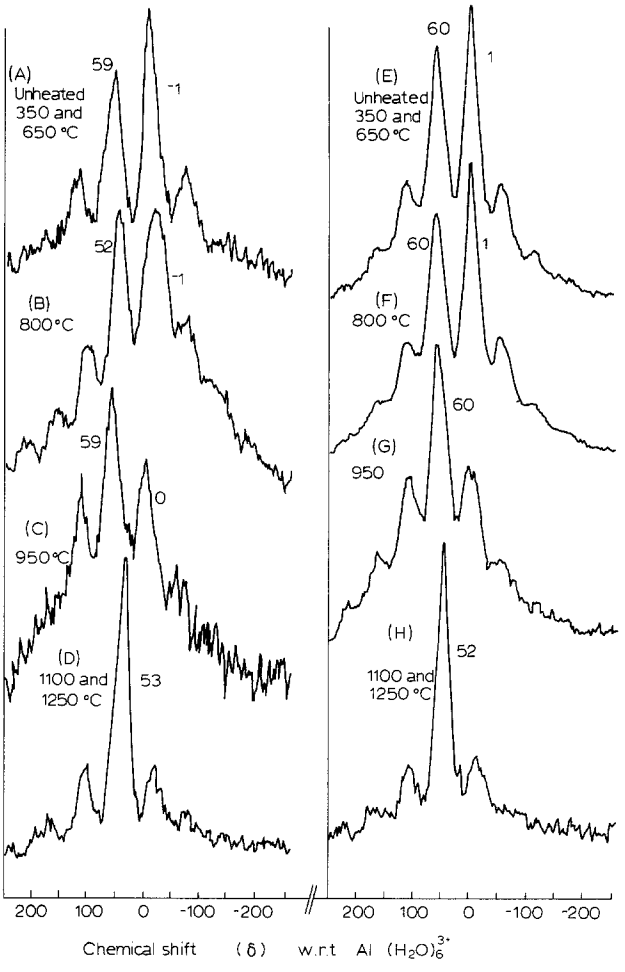

Figure 6 Typical ^{27}Al NMR spectra of muscovites heated to various temperatures. (A to D) Stewart Island muscovite, (E to K) North Carolina muscovite.

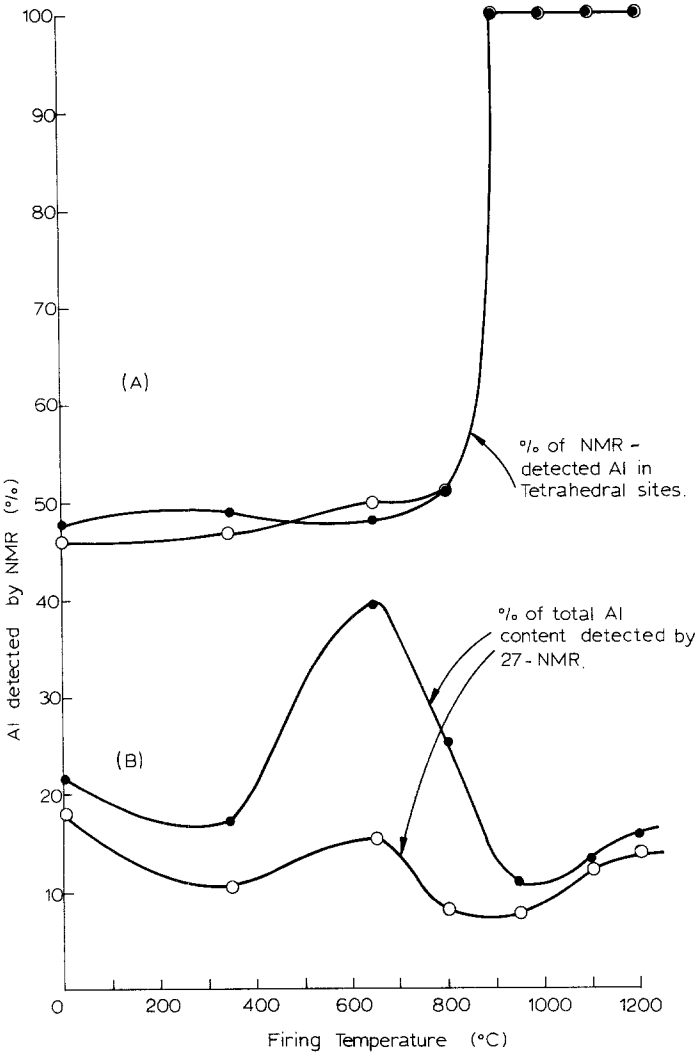

Figure 7 Effect of heating temperature on (A) the relative proportion of tetrahedral aluminium detectable by ^{27}Al NMR and (B) the proportion of the total aluminium detectable. (○) Stewart Island muscovite, (●) North Carolina muscovite.

In summary, the ^{27}Al NMR results suggest:

(a) fully dehydroxylated muscovite (heated at 950° C) contains, in addition to the aluminium in sites not detected by NMR (probably 5-coordinated), a proportion of 4-coordinated aluminium; since the chemical shift of this site is identical to that of the unheated material, it probably represents the aluminium in the original muscovite tetrahedral layer which is relatively unchanged by dehydroxylation.

(b) on recrystallization of the high-temperature phases the tetrahedral ^{27}Al chemical shift abruptly assumes a value found in potassium feldspars, suggesting that the feldspar-like phase forms directly from the tetrahedral layer, without free silica intermediates,

(c) ^{27}Al NMR provides no information about the formation mechanism of mullite or corundum, since octahedral aluminium present in these phases is not detected, possibly because they contain most of the impurity iron atoms.

3.3. Mössbauer spectroscopy

Typical room temperature Mössbauer spectra of the two muscovites, both heated and unheated, are shown in Fig. 8. The relative intensities of the doublet components vary slightly with the incident angle of the γ-ray beam due to orientation effects, as would be expected with mica samples. The spectra shown here were all obtained at normal incidence, with allowance made for non-equal dips, where appropriate, in the fitting procedure. The spectra of the unheated materials (Fig. 8A and E) can be computer-fitted to one Fe^{3+} and two Fe^{2+} doublets, as previously reported [26]. The isomer shift (IS) and quadrupole splitting (QS) parameters of the present Fe^{2+} sites a and b (QS = 3.02–3.07, IS = 1.13–1.15 mm sec^{-1} and QS = 2.10–2.24, IS = 0.98–1.12 mm sec^{-1}) are in reasonable agreement with previously reported values (QS = 2.87–3.08, IS = 1.09–1.15 mm sec^{-1} and QS = 2.14–2.28, IS = 1.10–1.15 mm sec^{-1}) [24–30]. The literature generally assigns the wider-QS resonance to the less-distorted *cis*-sites [24–30]. The present octahedral Fe^{3+} parameters of c are more influenced by the fitting philosophy adopted than are the Fe^{2+}; if the dips are not constrained to be equal, the parameters fall within the range quoted by other workers (QS = 0.66–0.73, IS = 0.34–0.42 mm sec^{-1} [24–30]. From a structural chemistry point of view, some substitution of tetrahedral Al by Fe^{3+} would be expected, but the present data are not sufficiently good for a tetrahedral Fe^{3+} doublet to be clearly necessary, even though such a doublet can be fitted.

Little change occurs in the spectra of samples heated below 650° C, but the onset of dehydroxylation at 800° C is accompanied by the disappearance of the wider-QS Fe^{2+} resonance a. The changes in site occupancy with heating temperature are summarized in Fig. 9. In samples fully dehydroxylated at 950° C,

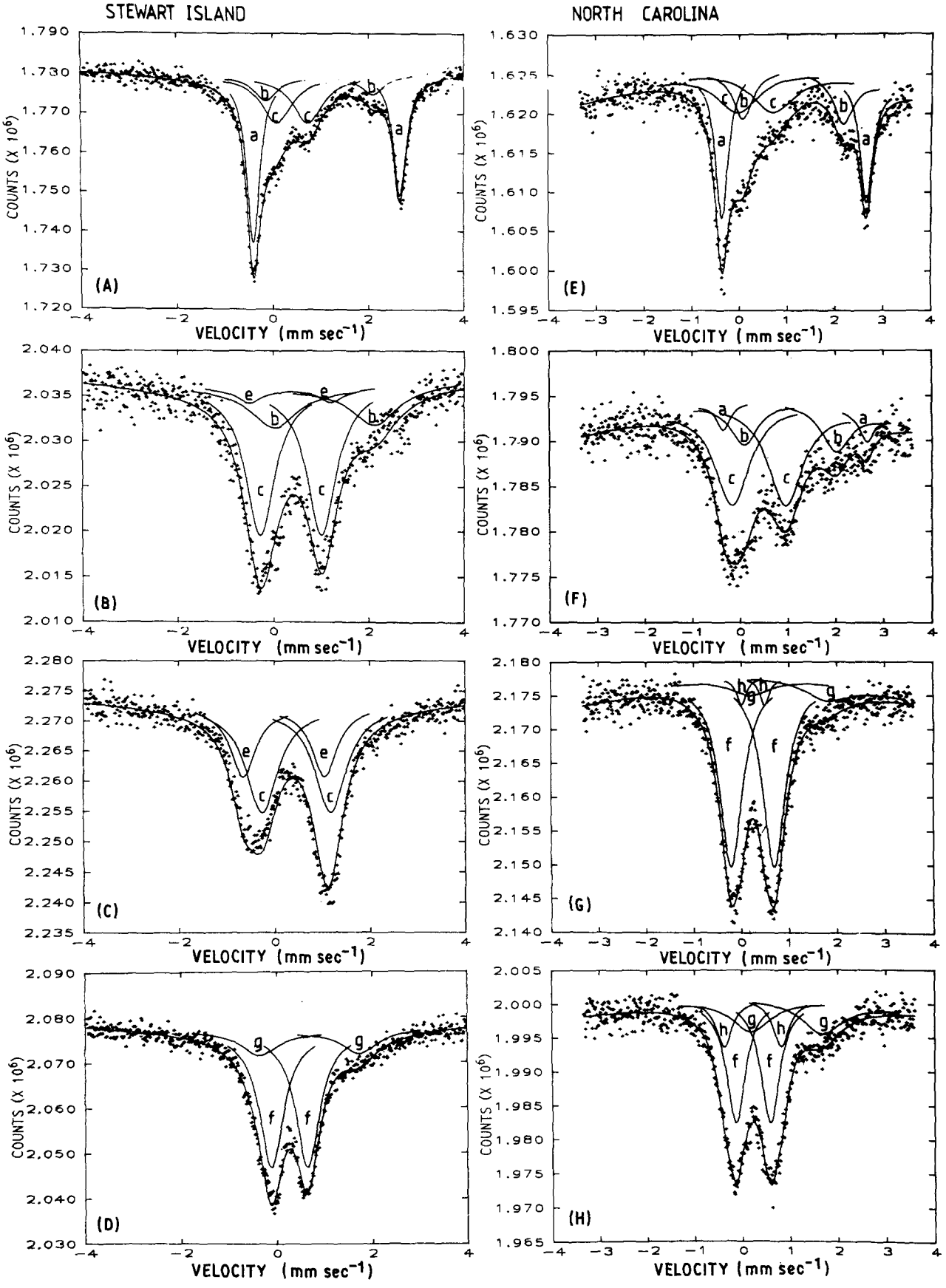

Figure 8 Typical room-temperature Mössbauer spectra of unheated and heated muscovites. (A to D), Stewart Island, (E to H) North Carolina. (A) Unheated–650° C, (B) 800° C, (C) 950° C, (D) 1100–1250° C, (E) unheated–650° C, (F) 800° C, (G) 1100° C, (H) 1250° C.

the more thermally stable narrower-QS Fe^{2+} resonance b has oxidized, with a concomitant change in the major Fe^{3+} doublet c, the parameters of which become QS = 1.24–1.44, IS = 0.36–0.46 mm sec^{-1}, similar to those found in montmorillonite dehydroxylate (QS = 1.21–1.28, IS = 0.34–0.36 mm sec^{-1} [8]) and tentatively attributed to Fe^{3+} in 5-coordinated sites [8]. The more iron-rich Stewart Island dehydroxylate also exhibits an additional transitory Fe^{3+} resonance e of similar parameters to one found in montmoril-

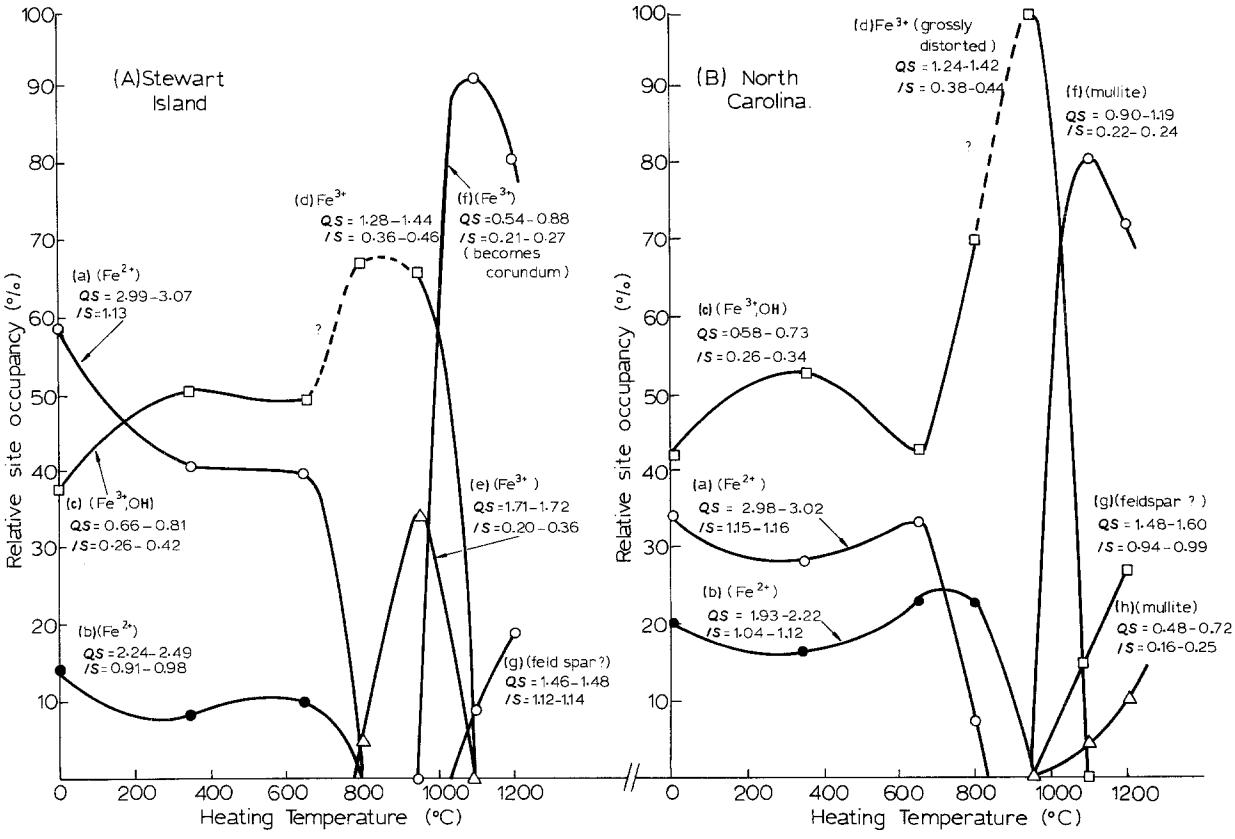

Figure 9 Changes in the relative site occupancy with heating temperature, deduced from the Mössbauer peak areas. Isomer shift values (*IS*) relative to natural iron.

lonite dehydroxylate [8] in which it was assigned to a distorted octahedral site. The destruction of the dehydroxylate and recrystallization of new phases at 1100° C is accompanied in both muscovites by the appearance of two new resonances f and g (Fig. 9). The similarity of the spectra at this stage is consistent with the X-ray observation of a spinel as the sole crystalline phase in both micas. However, even at 1100° C some differences are evident between the two muscovites, namely, (i) the Fe^{3+} sites in the North Carolina sample are more distorted than in the Stewart Island sample, having significantly larger *QS* values, (ii) the inclusion of a third doublet h, identified with a mullite resonance, improves the fit of the North Carolina spectrum but not the Stewart Island spectrum, from which it was therefore omitted. On heating at 1250° C for progressively longer times, further differences become apparent between the two muscovites. In North Carolina samples, the spectra remain virtually unchanged. The parameters of doublets f and h are similar to those found for a number of clay-derived and synthetic mullites (*QS* = 1.17–1.40, *IS* = 0.28–0.37 mm sec^{-1}, major resonance, and *QS* = 0.63–1.08, *IS* = 0.27–0.38 mm sec^{-1}, minor resonance) [31]. The parameters of doublet g are somewhat similar to a resonance found in an Fe^{3+}-containing feldspar synthetically recrystallized in a hydrothermal pressure vessel from an obsidian (volcanic glass) (unpublished results).

By contrast, the Stewart Island spectra change on heating at 1250° C as follows:

(i) The *QS* of doublet f progressively decreases, the final value (0.54 mm sec^{-1}) coinciding with those found in a series of synthetic corundum samples (*QS* = 0.52–0.55, *IS* = 0.27–0.34 mm sec^{-1}) [32].

(ii) Two new resonances appear – a doublet (*QS* = 0.33, *IS* = 1.24 mm sec^{-1}) and a singlet (*IS* ≈ 0), the parameters of which agree well with those of synthetic corundums [32].

(iii) Resonance g is replaced by a broad new resonance (*QS* = 2.09–2.28, *IS* = 0.69–0.73 mm sec^{-1}), similar to that found in feldspar synthetically derived from obsidian by hydrothermal treatment.

In summary, the Mössbauer results indicate:

(a) dehydroxylation of both muscovites results in resonances similar to those found in montmorillonite dehydroxylate, including one doublet tentatively attributed to Fe^{3+} in 5-coordinated sites.

(b) immediately on recrystallization (initially to a cubic phase), both muscovites develop spectra with at least one major resonance similar to that of mullite and a minor resonance similar to Fe^{3+} in feldspar. The lower-iron muscovite retains this spectrum on further heating, with a minor feldspar component.

(c) Of the iron content, 75–80% in both muscovites remains in the mullite or corundum phases, the remainder being associated with the feldspar phase.

4. Conclusions

1. The X-ray and solid-state NMR data for both the present samples are consistent with the structure of muscovite dehydroxylate proposed by Udagawa *et al.* [3], with a slightly modified tetrahedral layer containing both silicon and aluminium. ^{27}Al NMR provides no direct information about the fate of the octahedral cations, but Mössbauer spectroscopy of the sub-

stituent iron impurities suggests an extremely distorted environment similar to that of montmorillonite dehydroxylate. The present data appear more consistent with the homogeneous reaction mechanism of Eberhart [2], but an inhomogeneous mechanism cannot be ruled out on the basis that no octahedral aluminium is detected in the dehydroxylate, in view of the problems in detecting the ^{27}Al NMR signals from the octahedral regions of the high-temperature phases. This is probably due to the presence of iron in those sites, or large electric field gradients due to site distortions.

2. In both the higher-iron and lower-iron samples, the dehydroxylate decomposes by separation of the tetrahedral layers, which, with the interlayer K^+, forms a feldspar-like phase related to leucite, without separation of free silica. The remainder of the structure forms a spinel as previously reported, [2] but the ^{29}Si NMR suggests that it contains little silicon. The spinel cell parameter is consistent with that of γ-Al_2O_3, but the presence of iron (and probably magnesium) in this phase rules out direct confirmation by ^{27}Al NMR.

3. In both the present samples the spinel transforms initially into a highly aluminous mullite, and, in the higher-iron sample, corundum. This transformation occurs less readily in the low-iron sample, in which some corundum also temporarily appears at a later stage. Although some of the iron is located in the feldspar-like phase, it occurs predominantly in the aluminous phase, in which its action is to enhance the formation of corundum at the expense of mullite in the higher-iron sample. On prolonged heating, the mullite becomes more silica-rich by reaction with the feldspar-like phase.

Acknowledgements

We are indebted to Dr W. A. Watters, NZ Geological Survey, and Professor R. Roy, Pennsylvania State University for supplying the muscovite samples studied here, and to Dr C. W. Childs, Soil Bureau, DSIR, for the use of the Cryophysics Mössbauer

References

1. N. H. BRETT, K. J. D. MACKENZIE and J. H. SHARP, *Quart. Revs. Chem. Soc.* **24** (1970) 185.
2. J. P. EBERHART, *Bull. Soc. Franc. Mineral. Crist.* **86** (1963) 213.
3. S. UDAGAWA, K. URABE and H. HASU, *Ganseki Kobutsu Kosho Gakkaishi* **69** (1974) 381.
4. A. W. NICOL, "Clays and Clay Minerals", in Proceedings of the 12th National Conference on Clays and Clay Minerals, Atlanta, 1963, edited by W. F. Bradley (Pergamon, Oxford, 1964) p. 11.
5. N. SUNDIUS and A. M. BYSTROM, *Trans. Brit. Ceram. Soc.* **52** (1953) 632.
6. G. W. BRINDLEY, in "Progress in Ceramic Science, Vol. 3", edited by J. E. Burke (Pergamon, Oxford, 1963) p. 1.
7. K. J. D. MACKENZIE, I. W. M. BROWN, R. H. MEINHOLD and M. E. BOWDEN, *J. Amer. Ceram. Soc.* **68** (1985) 266.
8. I. W. M. BROWN, K. J. D. MACKENZIE and R. H. MEINHOLD, *J. Mater. Sci.*
9. R. C. MACKENZIE (ed) in "The Differential Thermal Investigation of Clays" (Mineralogical Society Monograph, London, 1957) Ch. 6.
10. W. E. CAMERON, *Bull. Am. Ceram. Soc.* **56** (1977) 1003.
11. A. MUAN and C. L. GEE, *J. Amer. Ceram. Soc.* **39** (1956) 207.
12. I. W. M. BROWN, K. J. D. MACKENZIE, M. E. BOWDEN and R. H. MEINHOLD, *ibid.* **68** (1985) 298.
13. J. SANZ and J. M. SERRATOSA, *J. Amer. Chem. Soc.*, **106** (1984) 4790.
14. E. LIPPMAA, M. MAGI, A. SAMOSAN, G. ENGELHARDT and A. R. GRIMMER, *ibid.* **102** (1980) 4889.
15. R. A. KINSEY, R. J. KIRKPATRICK, J. HOWER, K. A. SMITH and E. OLDFIELD, *Amer. Mineral.* **70** (1985) 537.
16. C. P. HERRERO, J. SANZ and J. M. SERRATOSA, *J. Phys. C: Solid State Phys.* **18** (1985) 13.
17. R. J. KIRKPATRICK, R. A. KINSEY, K. A. SMITH, D. M. HENDERSON and E. OLDFIELD, *Amer. Mineral.* **70** (1985) 106.
18. B. L. SHERRIFF and J. S. HARTMAN, *Can. Mineral.* **23** (1985) 205.
19. E. W. RADOSLOVICH, *Acta Crystallogr.* **13** (1960) 919.
20. N. GÜVEN, *Z. Krist.* **134** (1971) 196.
21. S. M. RICHARDSON and J. W. RICHARDSON, *Amer. Mineral.* **67** (1982) 69.
22. S. MOTHERWELL, "PLUTO", A Programme for Plotting Molecular and Crystal Structures" (University Chemical Library, Cambridge, England, 1976).
23. J. SANZ and J. M. SERRATOSA, *Clay Mineral.* **19** (1984) 113.
24. P. J. MALDEN and R. E. MEADS, *Nature* **215** (1967) 844.
25. L. H. BOWEN, S. B. WEED and J. G. STEVENS, *Amer. Mineral.* **54** (1969) 72.
26. C. S. HOGG and R. E. MEADS, *Mineralog. Mag.* **37** (1970) 606.
27. B. A. GOODMAN, *Mineralog. Mag.* **40** (1976) 513.
28. H. ANNERSTEN and U. HALENIUS, *Amer. Mineral.* **61** (1976) 1045.
29. T. ERICSSON, R. WAPPLING and K. PUNAKIVI, *Geol. Foeren. Stockholm Foerh.*, **99** (1977) 229.
30. J. FINCH, A. R. GAINSFORD and W. C. TENNANT, *Amer. Mineral.* **67** (1982) 59.
31. C. M. CARDILE, I. W. M. BROWN and K. J. D. MACKENZIE, submitted to *J. Mater. Sci. Lett.* **22** (1987) 357.
32. I. W. M. BROWN, K. J. D. MACKENZIE and C. M. CARDILE, *J. Mater. Sci. Lett.* **22** (1987) 535.

Received 8 September
and accepted 12 November 1986